Chapter 7
Freshwater Storage in the Northern Ocean and the Special Role of the Beaufort Gyre

Eddy Carmack[1], Fiona McLaughlin[1], Michiyo Yamamoto-Kawai[1], Motoyo Itoh[2], Koji Shimada[2], Richard Krishfield[3], and Andrey Proshutinsky[3]

7.1 Introduction

As part of the global hydrological cycle, freshwater in the form of water vapour inexorably moves from warm regions of evaporation to cold regions of precipitation and freshwater in the form of sea ice and dilute seawater inexorably moves from cold regions of freezing and net precipitation to warm regions of melting and net evaporation. The global plumbing that supports the ocean's freshwater loop is complicated, and involves land–sea exchanges, geographical and dynamical constraints on flow pathways as well as forcing variability over time (cf. Lagerloef and Schmitt 2006). The Arctic Ocean is a central player in the global hydrological cycle in that it receives, transforms, stores, and exports freshwater, and each of these processes and their rates both affect and are affected by climate variability. And within the Arctic Ocean, the Canada Basin (see Fig. 7.1) is of special interest for three reasons: (1) it processes freshwater from the Pacific, from North American and Eurasian rivers and from ice distillation; (2) it is the largest freshwater storage reservoir in the northern oceans; and (3) it has exhibited changes in halocline structure and freshwater storage in recent years.

In this chapter we examine the distribution of freshwater anomalies (relative to a defined reference salinity) in northern oceans by reviewing criteria that have been used to construct freshwater budgets and then by comparing freshwater disposition in the subarctic Pacific, subarctic Atlantic and Arctic oceans. This comparison provides a useful basis for the interpretation of Arctic Ocean flux measurements and affirms that the Canada Basin is a significant freshwater reservoir (Section 7.2). We next examine various hydrographic data sources within the Canada Basin (a geographical feature) to define the role of the Beaufort Gyre (a wind-forced dynamical feature) in freshwater storage and release (Section 7.3). Due to this latter feature, the upper

[1] Fisheries and Oceans Canada, Institute of Ocean Science, 9860 W. Saanich Road, Sidney, B.C., V8L 4B2

[2] Japan Agency for Marine-Earth Science and Technology, Yokohama, Japan

[3] Woods Hole Oceanographic Institution, Woods Hole, MA, USA

R.R. Dickson et al. (eds.), *Arctic–Subarctic Ocean Fluxes*, 145–169

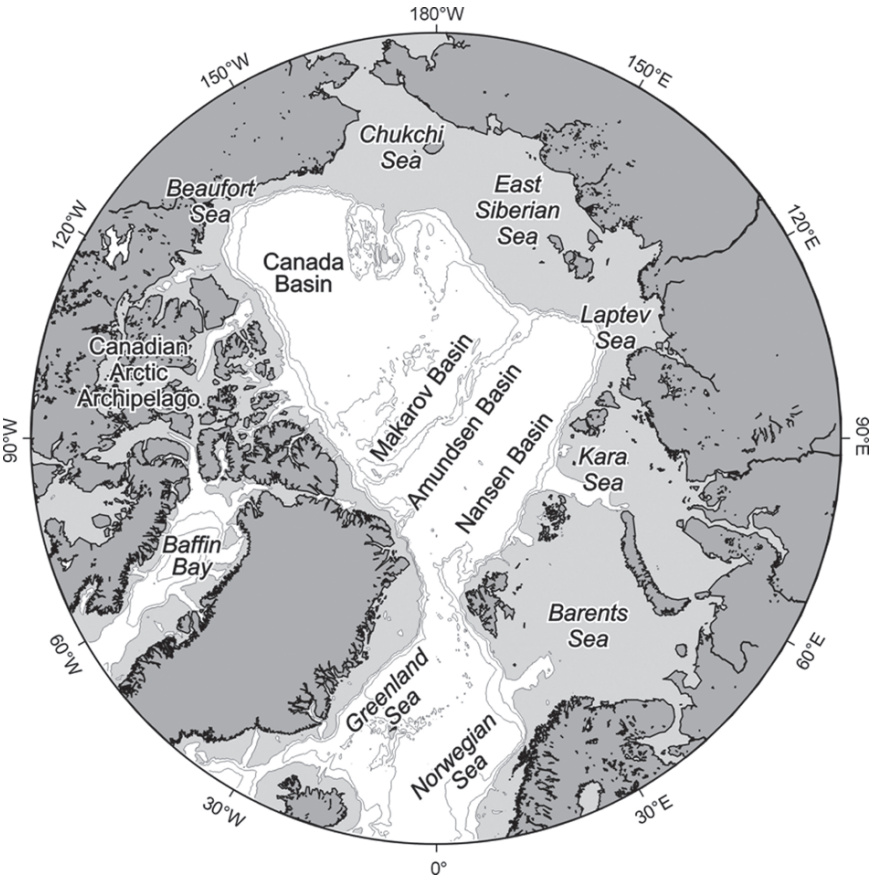

Fig. 7.1 Map of the study area

layer circulation in the Beaufort Gyre is anticyclonic whereas circulation elsewhere in the Arctic Ocean is cyclonic. Then we examine the Canada Basin's role as a reservoir with respect to sources of its freshwater components (e.g. meteoritic (runoff and precipitation), sea-ice melt and Pacific throughflow), and also to its water mass structure, within which freshwater components are stored (Section 7.4). This distinction among source components and among water mass affiliations is a prerequisite to interpreting downstream freshwater fluxes and to predicting the response of the Arctic system to climate variability. Finally, we combine geochemical data and recent freshwater budget estimates to calculate the relative contributions of freshwater components from the Canada Basin to other Arctic basins (Section 7.5). A summary and outlook is given in Section 7.6.

7.2 Freshwater Anomaly Definition

The first step in formulating freshwater budgets lies in defining a useful measure of freshwater content. The standard method defines a "freshwater anomaly", based on the selection of a defined reference salinity. This approach has often been used to construct budgets of confined seas and has the advantage that it relates directly to stratification which, in turn, constrains the dynamics of the system. The challenge, however, is to select an appropriate reference salinity. One method supposes a stirred box system and the freshwater anomaly is calculated with respect to a mean salinity within the box (Fig. 7.2a); for example, Aagaard and Carmack (1989) chose a reference salinity S = 34.8 for the Arctic Ocean. Alternatively the salinity of the saline end-member entering the confined sea is selected; for example, Dickson et al. (2007) chose S = 35.2 to represent the salinity of inflowing Atlantic water. Another strategy supposes estuarine circulation in the confined sea and here the reference salinity is chosen to be that of the lower layer which forms the base of the halocline (Fig. 7.2b). This approach was employed by Tully and Barber (1960) who used S = 33.8 to estimate the quantity of freshwater stored in the upper layers of the north Pacific, north of the subarctic front.

The weakness of the reference salinity approach becomes evident however, when ocean basins are not confined but are connected via sills and passageways. Thus an appropriate choice for one basin may be meaningless for the adjoining basin. Here it may be necessary to define a "practical" reference salinity for the upstream basin based on the salinity it can export above sill depth (Fig. 7.2c). Fortunately, budget calculations within a given confined basin (e.g. the Arctic Mediterranean) are not overly sensitive to small differences in the choice of reference salinity. Alternative approaches that are independent of a reference salinity have been advanced by Wijffels et al. (1992), who constructed a global budget for total freshwater, and by Walin (1977), who formulated conservation equations for an

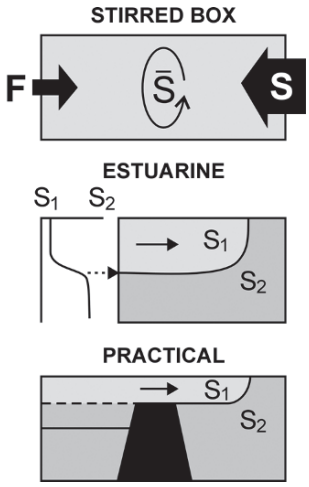

Fig. 7.2 Schematic showing various approaches used to define reference salinity

estuarine system using salinity and time as independent variables (natural coordinates). All of these approaches have merits and limitations and a choice must be based on intent and application.

An initial perspective on freshwater storage in the northern oceans can be obtained by mapping the distribution of salinity in arctic and subarctic seas at selected sill depths from climatological data (Conkright et al. 2002; World Ocean Data (WOD) 2001). The map of salinity at 20 m (Fig. 7.3a), taken to represent the salinity of the near-surface mixed-layer, shows that the Pacific at this depth is much fresher than the Atlantic ($\Delta S \sim 2$) and this low salinity water enters the Arctic Ocean through Bering Strait. Saline water from the North Atlantic crosses the Iceland–Scotland Ridge, flows northward through the Norwegian Sea and branches into the Barents and Greenland seas. Together these two sources define the large-scale estuarine forcing of the Arctic Ocean (cf. Stigebrandt 1984). The freshest near-surface water is found in the Canadian Basin (which includes both the Makarov and

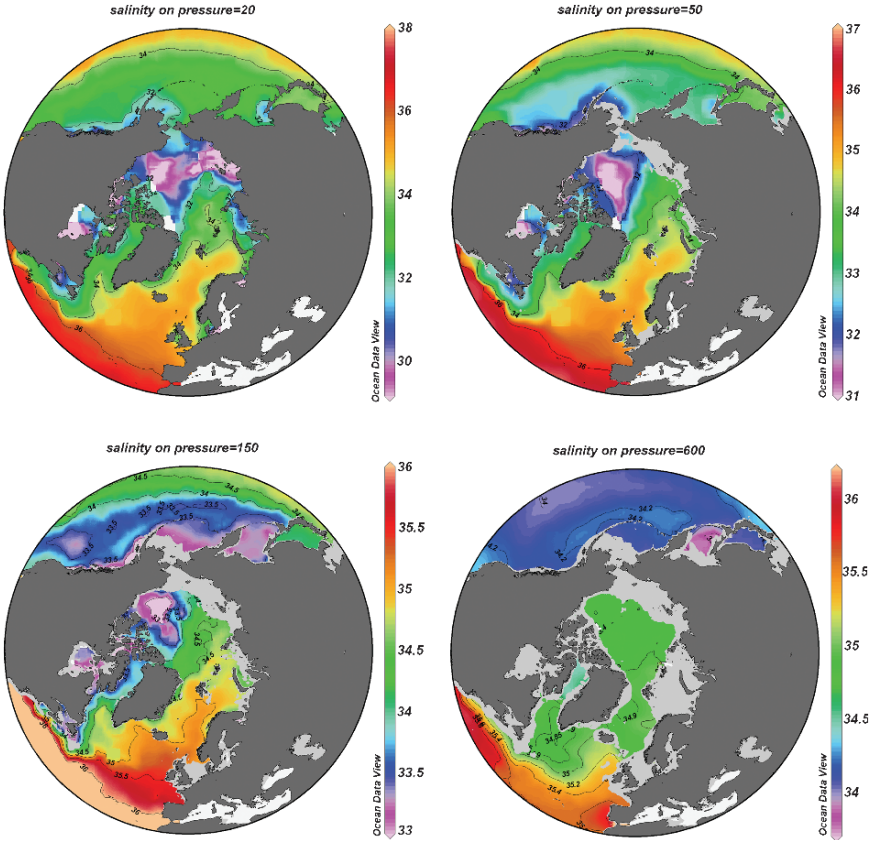

Fig. 7.3 Maps created from WOD 2001 showing the horizontal distribution of (a) salinity at 20 m, (b) salinity at 50 m, (c) salinity at 150 m and (d) salinity at 600 m

Canada basins) and is separated from a more saline upper layer found in the Eurasian Basin (Nansen and Amundsen basins) by a primary front that defines the baroclinic structure of the Transpolar Drift. The very low salinity waters lying above the East Siberian and Laptev seas, associated with Russian river inputs, are proximal to the western Canada Basin. Also evident are low salinity sources in the Kara Sea and southern Hudson Bay. The map of salinity at 50 m, the deepest depth connecting upper ocean waters of the Pacific, Arctic and Atlantic, defines the depth of free exchange of water masses among the three oceans (Fig. 7.3b). These two near-surface distributions of salinity also imply the key role of coastal-trapped and shelf-break currents in the transport of low salinity waters (cf. Griffiths 1986; Cenedese and Linden 2002; Williams et al. 2006; Bacon et al. 2007). (Because the resolution used in these mappings is insufficient to strictly distinguish between coastal-trapped and shelf break currents, we will use the term 'near-coastal flows in reference to them.') Such near-coastal flows are particularly fresh along the northeast Pacific, through the Canadian Archipelago and eastern coast of Canada and Greenland. Previous studies have demonstrated the regional importance of near-coastal flows forced by local freshwater discharge: for example, see Royer (1982) for the Northeast Pacific, Woodgate and Aagaard (2005) for the Bering Sea, McLaughlin et al. (2006) for the Canadian Arctic Archipelago, Chapman and Beardsley (1989) for the west coast of Greenland and Labrador Sea, and Bacon et al. (2002) for southern Greenland. Although no study has yet demonstrated the connectedness of these flows from a full, Northern Hemisphere perspective, we speculate that, jointly, such flows form a *contiguous* band of baroclinic flow around northern North America and constitute a substantial component of the freshwater transport (cf. Bacon et al., this volume, for the western subarctic Atlantic). The term contiguous reflects the fact that the forcing of individual components by freshwater inputs and wind is phased seasonally from one local current system to its downstream neighbour according to local supply of fresh water (cf. Carmack and McLaughlin 2001).

At 150 m (Fig. 7.3c), the approximate sill depth of passageways connecting the Arctic Ocean with the North Atlantic via the Canadian Archipelago, low salinity water is found almost exclusively within the Canada Basin. The fact that low salinity water is still evident at 150 m indicates how thick and therefore robust the reservoir of low salinity water in the Canada Basin is. The export pathway of these deeper, low salinity waters appears to be primarily through Nares Strait and the Canadian Archipelago. Salinity at 600 m (Fig. 7.3d), approximately the deepest depth connecting the Arctic Ocean with the global ocean via flow through Demark Strait, the Iceland–Scotland Ridge and Davis Strait, shows the relative uniformity of deep waters (S ~ 34.9) within the Arctic Ocean, Nordic Sea and Irminger Sea. The large-scale field of dynamic topography 20/600 dbar (Fig. 7.4, also see Steele and Ernold 2007) illustrates the 'downhill' journey, from Pacific to Arctic to the convective regions of the Nordic, Labrador and Irminger seas, that is largely responsible for sustaining arctic and subarctic fluxes.

One motivation for investigating freshwater distributions in high-latitude northern oceans lies in the dominant contribution of salinity to stratification. Stratification is

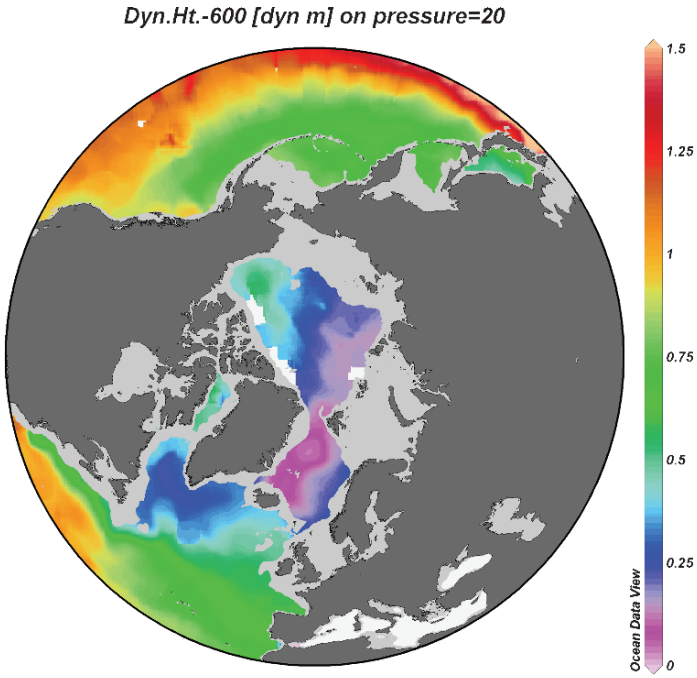

Fig. 7.4 Map showing dynamic topography (20/600 db)

typically expressed by the buoyancy frequency, $N^2 = g(d\rho/dz)$ where g is gravity and ρ is density. The density gradient can be further expressed as $d\rho/dz = \alpha(dT/dz) + \beta(dS/dz)$, where α is the thermal expansion coefficient, β is the haline contraction coefficient, dT/dz is the vertical gradient of temperature and dS/dz is the vertical gradient of salinity. Then $N^2 = N_T^2 + N_S^2$; where $N_T^2 = g\alpha(dT/dz)$ and $N_S^2 = g\beta(dS/dz)$. Because the magnitude of α decreases with decreasing temperature, the upper layers of the warm and saline subtropical seas are permanently stratified mainly by temperature; likewise the upper layers of cold, relatively fresh subarctic and arctic seas are permanently stratified mainly by salinity (cf. Carmack 2007). Because N_S^2 is, in fact, negative in subtropical seas, positive values of N_S^2 indicate freshwater storage. Thus the boundary defining the southern limit of salinity control on stratification and also the southern limit of freshwater storage in the upper ocean can be roughly identified by mapping the mean value of N_S^2 averaged between appropriate depth levels. Figure 7.5a, a map of N_S^2 averaged between 50 and 300 m, shows that the southern limit of salinity control roughly traces the boundary between the subtropical and subarctic gyres of both the Pacific and Atlantic oceans, and in the Atlantic it extends further northward into the Nordic Seas. High values of this stratification parameter are found in the Canada Basin and in western Baffin Bay. Moderately high values are found regionally in the North Pacific, in areas associated with Arctic outflow in the Canadian Archipelago, and along the east coast of Greenland. Moderately high values are also associated with river outflow in Hudson Bay and the Gulf of St. Lawrence.

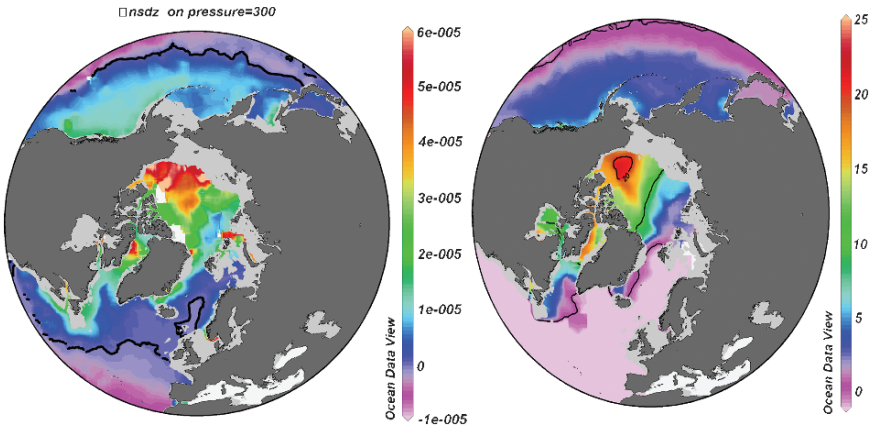

Fig. 7.5 Maps showing (a) the horizontal distribution of the contribution of salinity to mean stability $N_S^2 = g\beta(dS/dz)$ between 50 and 300 m, and (b) the freshwater equivalent height in northern oceans using the practical approach of selecting a reference salinity of 34.8 and using the following upstream sill depths: for Bering Strait (50 m); the Canadian Arctic Archipelago (150 m); Hudson Bay (100 m); and Denmark Strait (600 m). Although selective withdrawal over sills will occur, the use of upstream sill depth is useful as a first approximation. Black lines indicate freshwater equivalent heights of 0, 10 and 20 m

Based on the above discussion and incorporating the so-called practical approach of constraining the depth of integration depth according to 'upstream' sill depths for Bering Strait (50 m), the Canadian Arctic Archipelago (150 m), Hudson Bay (100 m) and Denmark Strait (600 m), the integrated freshwater content (equivalent height) relative to a reference salinity of 34.8 in the northern ocean is then calculated (Fig. 7.5b). From this figure it is evident that the North Pacific is a substantial upstream reservoir whose mean freshwater, expressed in equivalent height, is ~3–5 m (cf. Tully and Barber 1960; Aagaard et al. 2006). In contrast, the North Atlantic contains little freshwater apart from Arctic Ocean exit pathways. Within the Arctic Ocean the major reservoir of freshwater is the Canada Basin where 15–20 m is stored within the halocline and, moving toward the Atlantic, the equivalent height decreases from the Makarov (~10 m) to the Amundsen (~5 m) to the Nansen Basin (0–2 m). Given the magnitude of freshwater stored in the Canada Basin, changes in storage volume over time can significantly impact downstream fluxes and, at the same time, mask short-term imbalances in inflow and outflow rates.

7.3 Time Variability of Freshwater Storage in the Canada Basin

The volume of freshwater stored in the Arctic Ocean is roughly equal to that stored in all lakes and rivers of the world and is 10–15 times greater than the annual export of freshwater (including ice and water) from the Arctic Ocean (Aagaard and Carmack 1989). The bulk of this storage is located in the Canada Basin in association

with the anticyclonically driven and topographically steered Beaufort Gyre. Here, fresh water is accumulated by wind-forced Ekman convergence of low salinity waters from various proximal sources including Pacific inflow, river discharge and sea-ice melt (Proshutinsky et al. 2002). Hence the atmospheric forcing and mechanisms of air/ice/ocean coupling that affect its storage and release over time are of major importance. Proshutinsky et al. (2002) argued that the freshwater storage in the Beaufort Gyre varied according to the strength of anticyclonic wind-forcing in that freshwater would accumulate under strong anticyclonic forcing and would be released under weak forcing. Indeed, the release of only 5% of this freshwater could cause a change in the salinity in the North Atlantic similar to that of the Great Salinity Anomaly of the 1970s (Dickson et al. 1988). Based on changes in water mass distributions, the relative fresh water outflow between the Fram Strait and Canadian Arctic Archipelago gateways is now believed to vary on interannual timescales (McLaughlin et al. 2002; Steele et al. 2004; Falck et al. 2005). A detailed analysis of freshwater storage variability in the Arctic Ocean over the last 100 years has recently been completed by Polyakov et al. (2007). In this section we will briefly examine existing data for evidence of temporal variability, from multi-decadal to decadal to interannual, with focus on the Canada Basin and recognizing the limitations of the sparse historical data set.

We begin by looking for evidence of any large-scale changes in the distribution of freshwater within the Arctic Ocean over the past half century. For example, Swift et al. (2005) noted that the persistent (over several decades) wide-spread presence of Pacific water in the central Arctic Ocean halocline was followed by its abrupt disappearance from a large area in 1985 (also see McLaughlin et al. 1996). Decadal variability has been emphasized by Proshutinsky et al. (2005), Richter-Menge et al. (2006) and Polyakov et al. (2007). Accordingly, we examine freshwater content computed from gridded historical data from the 1950s to the 1980s (EWG) and

Table 7.1 List of expeditions

Year	Month	Expedition
1993	Aug.–Sept.	Scientific Ice Expedition (SCICEX)
1994	July–Aug.	Arctic Ocean Section
1995	May–Sept.	SCICEX
1996	Oct.–Sept.	SCICEX
1997	Oct.–Sept.	SCICEX
1997–1998	Oct.–Sept.	Surface Heat Budget of the Arctic Ocean/Joint Ocean Ice Study (SHEBA/JOIS)
1998	Aug.–Sept.	SCICEX
1999	Apr.–May	SCICEX
2000	Oct.	SCICEX
2002	Aug.–Oct.	Joint Western Arctic Climate Study (JWACS)
2003	Aug.–Sept.	JWACS/Beaufort Gyre Exploration Project (BGEP)
2004	Aug.–Oct.	JWACS/BGEP
2005	Aug.–Oct.	JWACS/BGEP
2006	Aug.–Oct.	JWACS/BGEP

from ship and submarine observations in the 1990s and 2000s (see Table 7.1) for evidence of decadal change in the Canada Basin. We note that data from the 1990s are sparse and there are no observations from 76–80° N along 140° W. The observational data are extracted every 0.5° from gridded fields produced by fitting a polynomial surface to the observations and smoothed slightly in latitude with a 1° running mean triangular filter. Sections along 140 and 150° W (Fig. 7.6) reveal no discernable decadal trend in the cumulative freshwater content from the 1950–1980s.

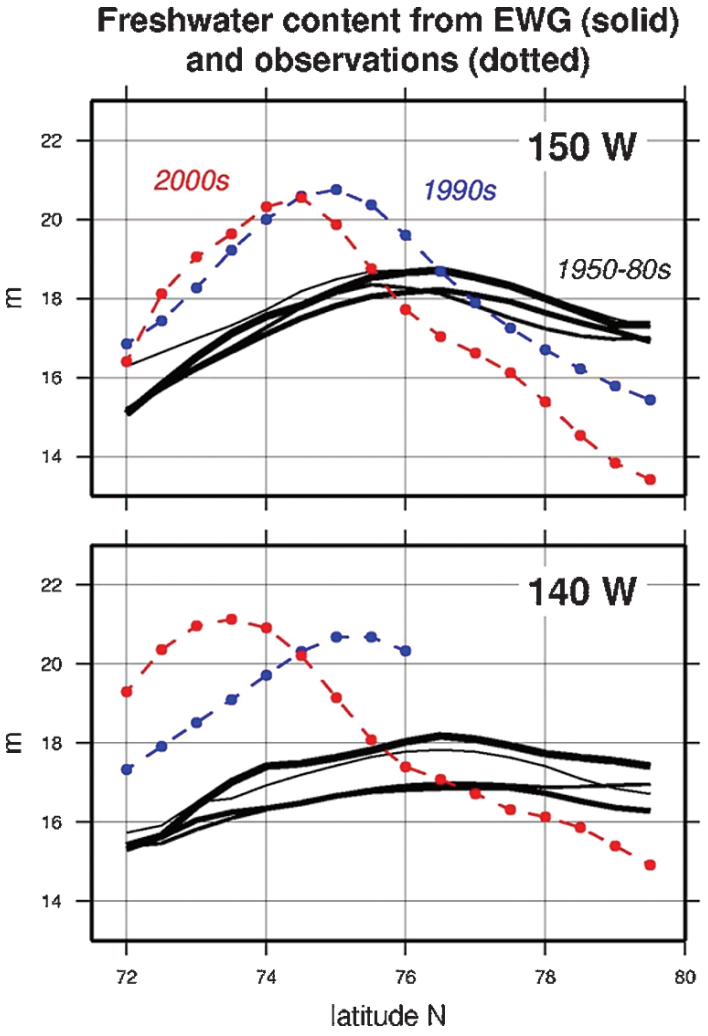

Fig. 7.6 Freshwater content computed from gridded historical data (EWG) from the 1950s to the 1980s, from ship and submarine expeditions in the 1990s and from the Canada /Japan/US Joint Western Arctic Climate Study in the 2000s. The black lines that represent the EWG data are thinnest in the 1950s and thickest in the 1980s

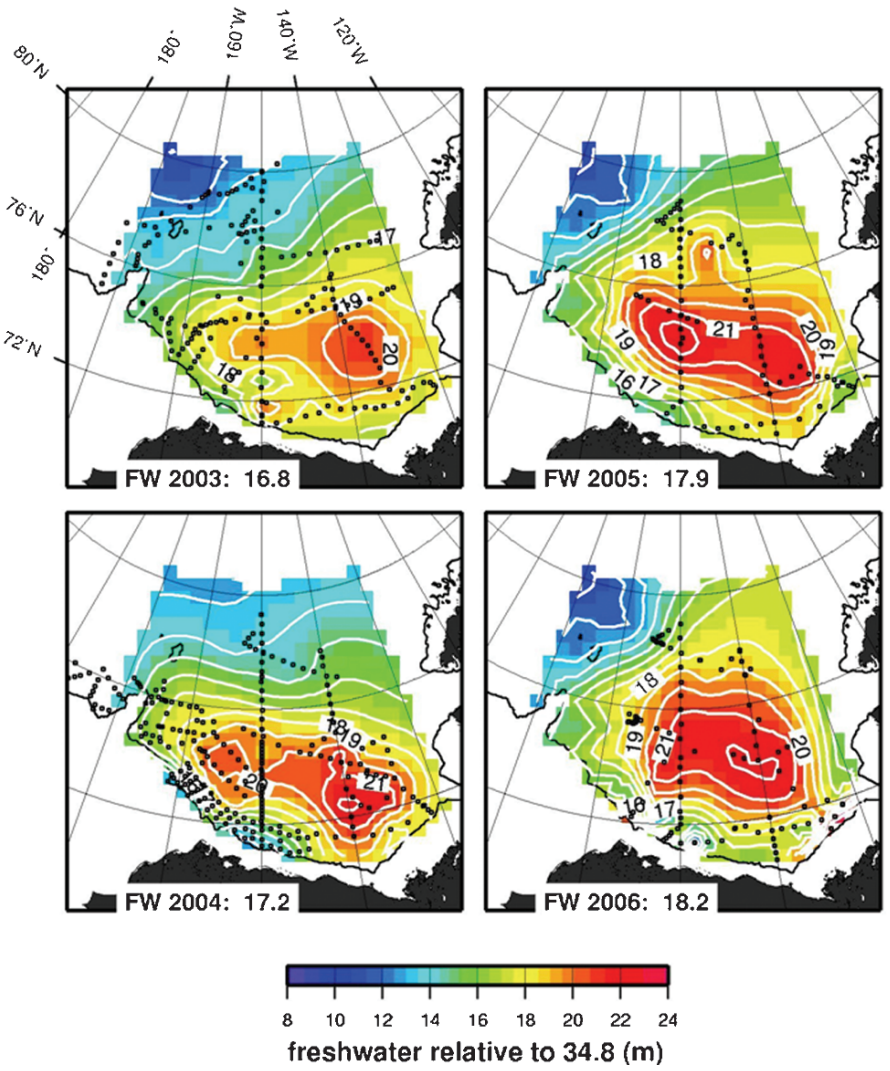

Fig. 7.7 Comparison of freshwater content in the Beaufort Gyre in (a) 2003, (b) 2004, (c) 2005 and (d) 2006. Numbers at the bottom of each figure indicate the total freshwater content in the gridded region (×1,000 km^3) for each year

In the 1990s, however, there was a shift in freshwater distribution, with an increase in freshwater content in the southern portions of the basin and a compensating decrease in the northern portion. In the early 2000s the freshwater content maximum shifted toward the east, away from the Northwind Ridge (near 150° W)

and southward towards Banks Island (near 140° W). We acknowledge that these temporal changes are speculative, as they may include spatial and seasonal variability due to data sparseness.

Finally we examine recent data (2003–2006) from the southern Canada Basin (south of 80° N) for evidence of interannual variability (Fig. 7.7). Maps of freshwater equivalent height show variability in the Beaufort Gyre, identified by freshwater equivalent heights of approximately 20 m. In 2002 (not shown), the gyre was located between 72° and 76° N and 140° and 150° W. In 2003 the gyre shifted slightly eastward by approximately 2–3°, however a secondary maximum in freshwater content remained along 150° W near 74° N. In 2004 the shape of the gyre is more elongated and two relative maxima are evident, the larger being near 73° N and 140° W (>22 m) and the smaller near 74° N and 155° W. In 2005 the core remains elongated, the region covered by 20 m is larger and the freshwater content maximum is located along 150° W. In 2006, the maximum again shifted eastward and the core of the gyre spread northward. Overall, the total freshwater content in the region appears to have increased slightly over this 5-year period. These recent data suggest interannual variability in the spatial distribution of freshwater and indicate that the Beaufort Gyre may be tightly coupled to interannual changes in wind forcing and air–sea-ice coupling (cf. Shimada et al. 2006).

7.4 Freshwater Components and Distributions in the Canada Basin

Thus far we have examined freshwater content by integrating the salinity anomaly relative to a reference salinity of 34.8, and have reported variability on a number of spatial and temporal scales. It is also important to understand where and how each freshwater *component* stored in the present ocean is derived to predict the effects of future change. Although the main approach used here identifies source constituents (i.e. meteoritic, sea-ice melt, Pacific), it is initially important to recognize freshwater storage on the basis of its water mass distributions (e.g. with the mixed layer, Pacific summer water, Pacific winter water, lower halocline). Stratification in the Canada Basin is especially complicated and the halocline is comprised of a series of layers (modes and clines) from the surface down to about 300 m (Fig. 7.8). The temperature and salinity structure is characterized by a seasonal mixed layer found in the upper ~40 m, wherein the effects of sea-ice melt and river plume spreading in summer and sea-ice formation in winter are manifest. Below, from ~40 to ~200 m, lie both summer and winter influxes of Pacific-origin water. Pacific-origin winter water is further characterized by high nutrient levels and a distinct N/P relationship. Below ~200 m the transition to Atlantic-origin waters occurs, first with the Lower Halocline layer which in turn overlies the Atlantic water.

Following from the seminal work of Östlund (1982) on $\delta^{18}O$ partitioning, a number of authors have applied this and other geochemical tracers to examine the constituents of Arctic Ocean freshwater by source (cf. Macdonald et al. (1995) used $\delta^{18}O$; Guay and Falkner (1997) used barium; Jones et al. (1998) used nitrate/phosphate

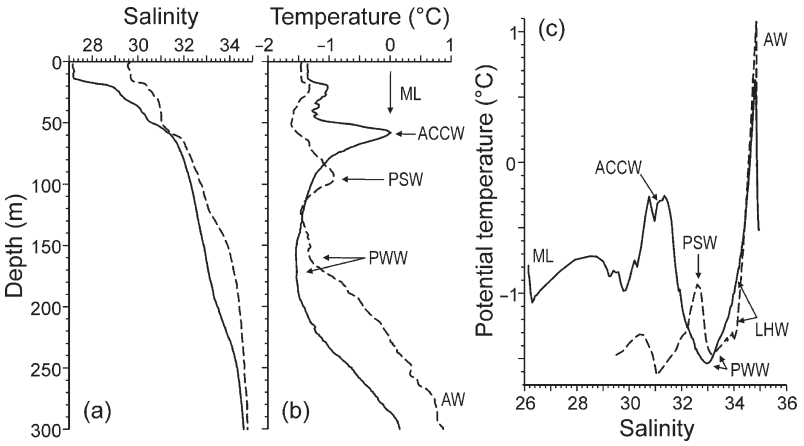

Fig. 7.8 Two representative stations from the Canada Basin illustrating regional water mass structure: (a) profile of salinity, (b) profile of temperature and (c) the corresponding θ/S correlation diagram. The winter mixed-layer (ML) extends to 40–50 m depth. A number of different Pacific-origin water masses are present: summer inflows include Alaska coastal current water (ACCW) that enters near Barrow Canyon, Pacific summer water inflows (PSW) and Pacific winter water (PWW). Atlantic-origin waters include lower halocline water (LHW); and the Atlantic layer (AW) which is comprised of Fram Strait branch waters indicated by the temperature maximum and Barents Sea branch waters (not shown)

relationships; Ekwurzel et al. (2001) used $\delta^{18}O$ and PO_4^*; Yamamoto-Kawai et al. (2005) used $\delta^{18}O$ and alkalinity). Additional refinements have been used to identify source origin, for example, Anderson et al. (1994) used alkalinity and silicate to distinguish between Pacific and river waters in the upper waters of the Eurasian Basin and Guay and Falkner (1994) used barium to distinguish between Eurasian and North American river discharge. Yamamoto-Kawai et al. (2005) showed that alkalinity and $\delta^{18}O$ are interchangeable tracers of freshwater and brine in the Arctic Ocean, with the exception in regions where waters are influenced by Mackenzie River discharge.

The main objective of such analysis is to partition a seawater sample into its primary constituents – meteoritic water, sea-ice melt and a meaningfully defined saline end-member – and this is typically done using $\delta^{18}O/S$ correlations. With regards to the saline end-member a number of different choices have been made. For example Macdonald et al. (1995) and Macdonald et al. (2002) used the polar mixed layer (S = 32.2) and middle halocline water (S = 33.1), respectively, although these layers are already diluted with sea-ice melt/brine and meteoric water. Melling and Moore (1995) and Yamamoto-Kawai et al. (2005) used Atlantic water as the saline end-member since Pacific water appears roughly as a mixture of Atlantic water and meteoric water on a $\delta^{18}O/S$ correlation diagram. However, this approach cannot distinguish Pacific water from meteoric water. Bauch et al. (1995) and Ekwurzel et al. (2001) used silicate and PO_4^*, respectively, to estimate the contribution of Pacific water because values are much higher in Pacific water than in

Atlantic water. As nutrients undergo significant seasonal variability while crossing the Bering and Chukchi seas this method may underestimate the contribution of Pacific water. To avoid these effects, Jones et al. (1998; 2003) used the nitrate–phosphate (N/P) relationship as a tracer of Pacific water. They noted that the N/P correlation diagram consists of three straight-line segments. Two near-parallel lines, that follow the Redfield ratio, represent Atlantic and Pacific sources and the offset between them arises from denitrification in Pacific inflow during transit across the Bering and Chukchi shelves. These two lines are connected by a third line that represents mixing between the superimposed Pacific and Atlantic water masses. Water at any point on this mixing line can thus be divided into its Atlantic and Pacific fractions. Yamamoto-Kawai et al. (2008) modified the Jones method and used dissolved inorganic nitrogen instead of nitrate so as to include the ammonium associated with regeneration and high production on the Chukchi Shelf. In the Canada Basin the mixing point line corresponds to salinities from S ~33.0 to ~34.8.

The most recent freshwater inventory of the Canada Basin, calculated by Yamamoto-Kawai et al. (2008) from data collected in 2003–2004, are used to investigate constituent distributions. They combined an analysis of N/P correlations, thus identifying the saline end-members, with an analysis of $\delta^{18}O/S$ correlations and a three component mixing model for meteoritic water, Sea-ice meltwater and saline end-member water, using the following approach. Pacific water is the saline end-member for $S \leq 33$ waters. In $S > 33$ waters, the saline end-member is a mixture of Pacific and Atlantic waters, and the mixing ratio is calculated using the Jones et al. (1998) approach (see Yamamoto-Kawai et al. 2008 for equation). Next, S and $\delta^{18}O$ values for the saline end-member are calculated using the fraction of Pacific water and values for inflowing Pacific-origin ($S = 32.5$, $\delta^{18}O = -0.80$) and Atlantic-origin water ($S = 34.87$, $\delta^{18}O = 0.24$, see Yamamoto-Kawai et al. 2007 for selection criteria). The three component mixing model is then applied to estimate freshwater fractions of meteoritic water, sea-ice melt and saline end-member components, and the saline end-member is further divided into its Pacific and Atlantic parts.

The resulting mean vertical distributions of freshwater components (calculated as the mean depth of a given fraction, $\langle \mathbf{Z}(f) \rangle$ for Pacific and Atlantic waters, and the mean fraction at a given depth $\langle \mathbf{f}(Z) \rangle$ for meteoritic and sea-ice melt components) computed from all stations deeper than 1,000 m are shown in Fig. 7.9. To further show the association of freshwater components with distinct water masses, these fractions are then plotted on a θ/S correlation diagram from each station in the Canada Basin (Fig. 7.10). The seasonal mixed layer ($S < \sim 31$, cf. Carmack et al. 1989) is mainly comprised of Pacific water (>80%), freshened by the addition of meteoric water (10–20%). Sea-ice melt slightly freshens (<10%) the upper 30 m of the seasonal mixed layer whereas the addition of brine (i.e. negative sea-ice melt) makes the lower 10–20 m more saline. The transition from freshening by melting to increasing the salinity by brine injection occurs above the base of the seasonal mixed layer at 30 m and S ~ 30. Summer and winter influxes of Pacific-origin water dominate (>80%) the water column to ~175 m and S ~ 33.3 and are greater than 70% to ~190 m and S ~ 33.8, the later being due to the injection of hypersaline polynya water (cf. Weingartner et al. 1998) and diapycnal mixing of Pacific water (Woodgate

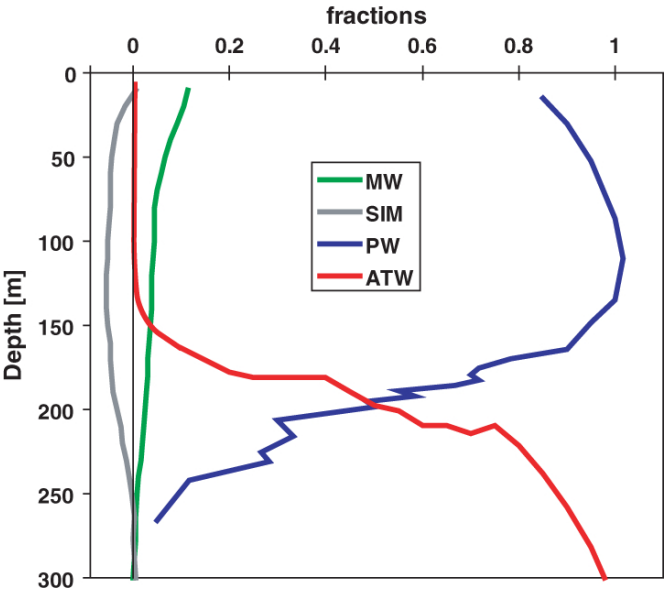

Fig. 7.9 The mean vertical profile of source water fractions in the Canada Basin 2003–2004: meteoric (MW), sea-ice melt water (SIM), Pacific water (PW) and Atlantic water (ATW). Only stations >1,000 m depth are used. Mean profiles are calculated as the mean fraction at a given depth <**Z**(f)> for MW and SIM, and the mean depth of a given fraction, <**f**(Z)> for PW and ATW

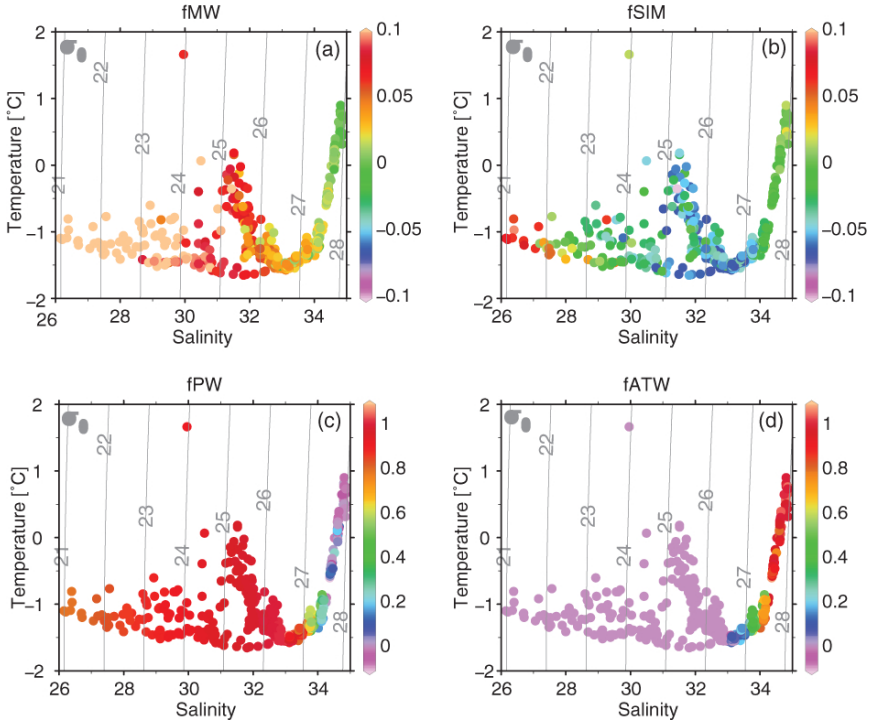

et al. 2005) into Lower Halocline Water. The transition to more than 80% Atlantic water occurs sharply and at ~220 m and S = 34.2. It is interesting to note that very small amounts of meteoric water and brine are present in both summer and winter Pacific waters and in Atlantic waters to S ~ 34.2. As there is no freshwater component below 300 m it is the depth of integration used in the following calculations.

Integrating the fraction of Pacific water at each station, the horizontal distribution of the equivalent thickness of Pacific water is calculated and when mapped is found to be >200 m in the south and <150 m in the north (Fig. 7.11a). The geographic difference in the depth of Pacific water corresponds to the apparent influx of Atlantic water around the northern perimeter of the Northwind Ridge by topographically steered boundary currents (Fig. 7.11b; also see McLaughlin et al. 2002; McLaughlin et al. 2004; Häkkinen and Proshutinsky 2004; Shimada et al. 2004) and spatial variability in Ekman pumping associated with the large-scale wind field and air/ice/sea/coupling (cf. Shimada et al. 2006).

To examine the horizontal distribution of freshwater by component, the freshwater equivalent fractions at every station are calculated using S = 34.87 as the reference salinity, integrated and mapped (see Yamamoto-Kawai et al. 2008 for selection of reference salinity and error analysis). It should be noted that use of S = 34.87 instead of S = 34.8 as a reference salinity results in a difference in integrated content of 1–2%. The equivalent thickness of total freshwater is ~20 m in the southeastern Canada Basin and decreases to ~14 m in the northwest (Fig. 7.12a). The equivalent thickness of meteoritic water is highest (>15 m) near the Mackenzie River and

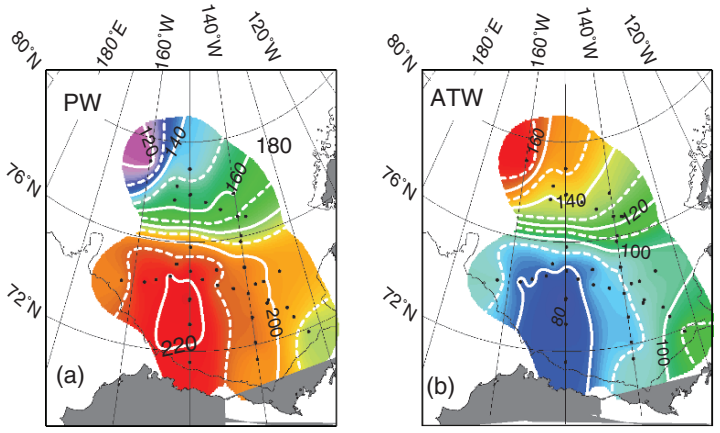

Fig. 7.11 Horizontal distribution of equivalent thickness of (a) Pacific water and (b) Atlantic water integrated from 0 to 300 m. Only stations >1,000 m depth are used

Fig. 7.10 Distribution of freshwater components plotted on a T/S correlation diagram; only stations >1,000 m depth are used: (a) fraction of meteoritic water; (b) fraction of sea-ice melt; (c) fraction of Pacific water; and (d) fraction of Atlantic water. Gray lines indicate isopycnal contours

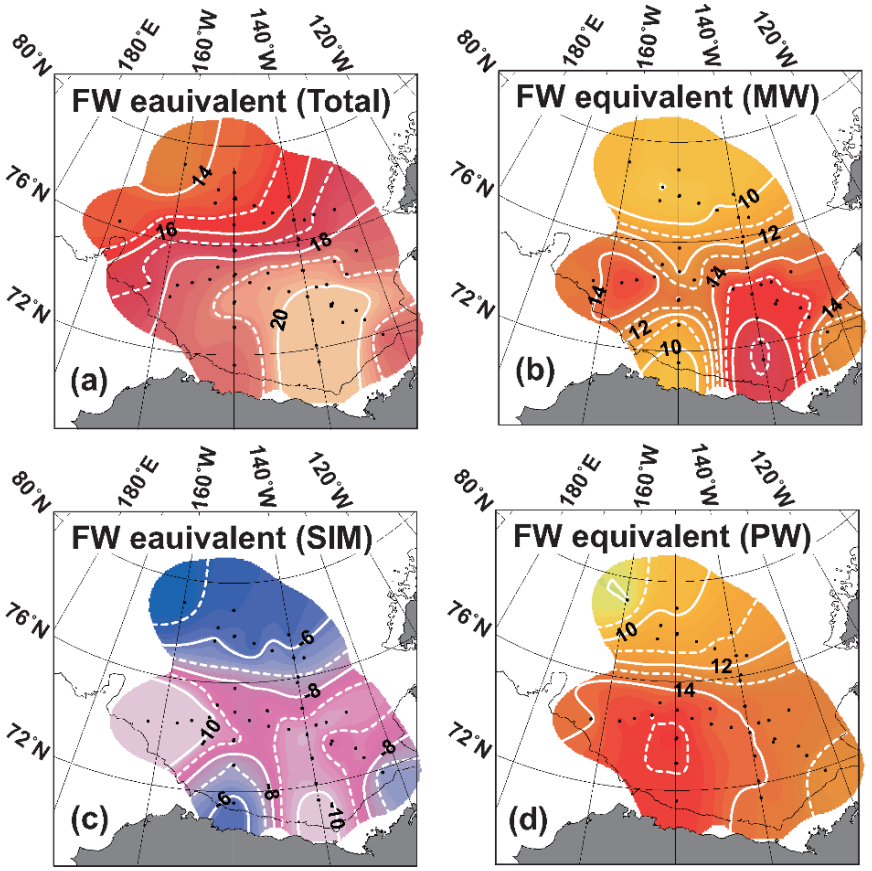

Fig. 7.12 Horizontal distribution of freshwater equivalent thickness of (a) total freshwater equivalent; (b) meteoritic water, (c) sea-ice melt; and (d) freshwater equivalent of Pacific water. Only stations >1,000 m depth are used

decreases to ~10 m in both the northwest and southwest (Fig. 7.12b). The equivalent thickness of sea-ice melt is negative throughout the basin and this indicates that freshwater is removed by sea-ice formation and net export from the Canada Basin (Fig. 7.12c). The equivalent thickness of freshwater removed as sea-ice is ~6 m in the north and ~9 m in the south with higher values (~10 m) near the northern Chukchi and Beaufort shelves and lower values (~6 m) near the coast at Point Barrow. However, as brine can be laterally transported into the basin by shelf-basin exchange mechanisms, the distribution of *net* sea-ice formation does not necessarily represent *in situ* ice formation but instead reflects the history of the water mass. The equivalent thickness of Pacific-origin freshwater is ~14 m in the south and ~10 m in the north (Fig. 7.12d). The mean inventories of meteoric water, the freshwater equivalent of sea-ice melt and the freshwater equivalent of Pacific water for

the study area are found to be 13 m, −8 m and 13 m, respectively. The mean for the entire Canada Basin is likely lower than this because the freshwater content in the northern part of Canada Basin is lower than in the southern part, and therefore values of 10.5 m, −6.5 m and 12 m – the mean freshwater inventories for the central Canada Basin (75–80° N) – are used in the calculations below (see Yamamoto-Kawai et al. 2008).

In summary, freshwater in the Canada Basin is comprised primarily of meteoric water and the freshwater equivalent of Pacific water, and they contribute almost equally to the total freshwater found in the upper 300 m. The net effect of sea-ice formation and melting is to remove ~30% of the freshwater contributed by both meteoric and Pacific water.

7.5 Freshwater Storage, Flux and Residence Time

7.5.1 Canada Basin

The mean freshwater inventories for the central Canada Basin (75–80° N) now can be used to calculate the storage, flux, and residence time of freshwater components (Fig. 7.13). Multiplying the mean freshwater inventories by the surface area of the

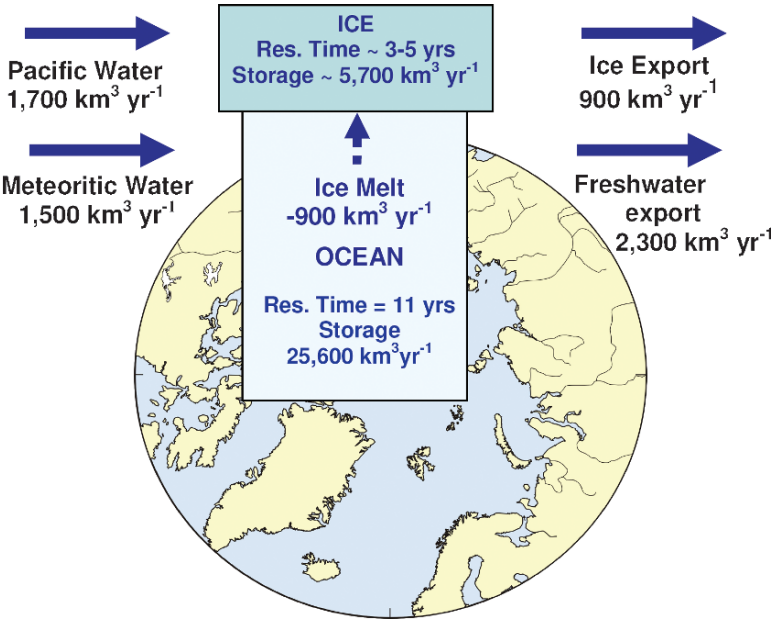

Fig. 7.13 Schematic of the freshwater budget for the Canada Basin

Canada Basin deeper than 1,000 m (1.6×10^6 km^2), the volumes of meteoritic and freshwater equivalent of Pacific water are computed to be 16,800 km^3 and 19,200 km^3, respectively, whereas 10,400 km^3 of freshwater have been removed by sea-ice export. The total (net) freshwater storage in the top 300 m of the Canada Basin is thus 25,600 km^3 and this corresponds to approximately one third of the total freshwater stored in the Arctic Ocean (Zhang and Zhang 2001). The volumes of meteoric water and freshwater equivalent of Pacific water actually stored in the ocean depend on the fractions of each of these freshwater sources that are removed as ice. Given that the water in the winter mixed-layer is approximately a 1:9 mixture of meteoric water and Pacific water, and assuming that sea-ice is formed equally from both sources, then the volume of meteoric water and freshwater equivalent of Pacific water actually stored is 15,800 and 9,800 km^3, respectively.

The addition of 19,200 km^3 of freshwater equivalent of Pacific water corresponds to approximately 11 years of Pacific inflow through Bering Strait, and this residence time is calculated as follows. The mean transport of water through Bering Strait is ~0.8 Sv with a mean salinity of S = 32.5 (Woodgate et al. 2005), supplying ~1,700 km^3 year^{-1} of freshwater (relative to S = 34.87) into the Arctic Ocean. Although the Alaskan Coastal Current (cf. Woodgate and Aagaard 2005) also carries ~700 km^3 year^{-1} of additional freshwater into the Canada Basin, this freshwater component will be included in the meteoric water component in our three component analysis. Assuming that all inflowing Pacific water enters the Canada Basin interior, the mean residence time in the upper 300 m is thus about 11 years (19,200 km^3/1,700 km^3 year^{-1}). Applying this residence time to the volumes of other stored components, the fluxes of meteoric water and freshwater equivalent of sea-ice melt are 1,500 km^3 year^{-1} (of this, ~700 km^3 year^{-1} enters through Bering Strait) and −900 km^3 year^{-1}, respectively. Admittedly the residence time of the near-surface layer, where the fractions of meteoric water and sea-ice melt are higher (see Fig. 7.10), is likely shorter than 11 years, and thus our estimates above represent lower limits of flux. This residence time estimate of 11 years is consistent with tritium–helium ages of < 4 years at the surface and ~18 years at 300 m (Smethie et al. 2000) and with tritium ages of 10–16 years of the freshwater component (Östlund 1982). Assuming that a mean thickness of sea-ice in the Canada Basin deeper than 1,000 m (1.6×10^6 km^2) is 2–3 m, and the salinity of sea-ice is S = 4, then the volume of freshwater stored in sea-ice in the Canada Basin is 2,800–4,300 km^3. Applying the sea-ice flux value, the residence time of sea-ice in the Canada Basin is 3–5 years (cf. Rigor and Wallace 2004).

7.5.2 Arctic Basin Export to the North Atlantic

We can now combine budgets constructed for the Canada Basin with published estimates of the boundary conditions for the Arctic Ocean (e.g. basin-wide estimates of river discharge, net precipitation and ice and liquid water export to the North Atlantic) to develop a rough budget for freshwater component fluxes in the whole arctic

basin. Estimates of river discharge, net oceanic precipitation and exports of ice and liquid freshwater through Fram Strait and the Canadian Arctic Archipelago are taken from Serreze et al. (2006), fluxes through Bering Strait are taken from Woodgate and Aagaard (2005) and fluxes of freshwater components into and out of the Canada Basin are taken from the above budget (also see Yamamoto-Kawai et al. 2008); this formulation, specific to the Canada Basin, is shown schematically in Fig. 7.13.

Now, to arrive at a budget for the entire Arctic Ocean, the region is divided into two principal domains: the Canada Basin and all other basins (Fig. 7.14). This distinction is physically relevant because it separates the halocline of the Arctic Ocean into its anticyclonic (Beaufort Gyre) and cyclonic (Trans Polar Drift) components. The freshwater equivalent of Pacific water that enters via Bering Strait is 1,700 km^3 $year^{-1}$, the total volume of runoff that enters the Arctic Ocean is 3,300 km^3 $year^{-1}$ and the net oceanic precipitation is 2,000 km^3 $year^{-1}$. The flux of meteoritic water into the Canada Basin is ~1,500 km^3 $year^{-1}$ and ~700 km^3 $year^{-1}$ of this enters through Bering Strait. Thus ~800 km^3 $year^{-1}$ of the total meteoritic influx (5,300 km^3 $year^{-1}$) should enter the Canada Basin and

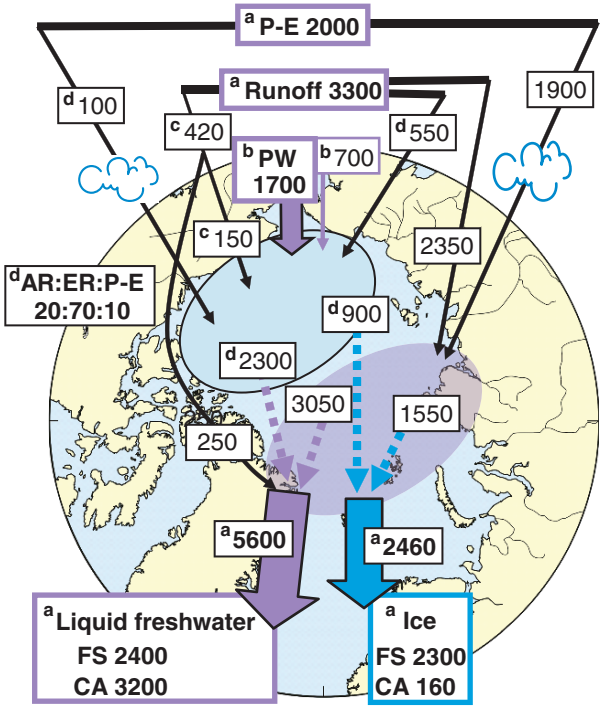

Fig. 7.14 Schematic of the freshwater budget of the Arctic Ocean, showing the partitioning of freshwater export. Superscripts indicate the references used flux values (km^3 $year^{-1}$): (a) is Serreze et al. 2006; (b) is Woodgate and Aagaard 2005; (c) is Lammers et al. 2001; and (d) is Yamamoto-Kawai et al. 2008

4,500 km^3 $year^{-1}$ must therefore enter into the other basins. Using the component ratios of meteoric water obtained by Yamamoto-Kawai et al. (2008: American Rivers: Eurasian Rivers: Net Precipitation = 20:70:10), and assuming accuracies of ±50 km^3 $year^{-1}$ in rates estimated here and Yamamoto-Kawai et al. (2008), then 150 km^3 $year^{-1}$ of the meteoric water in the Canada Basin is from the discharge of North American rivers and 550 km^3 $year^{-1}$ from Eurasian Rivers. This suggest that 250 km^3 $year^{-1}$ of total discharge from North American rivers (420 km^3 $year^{-1}$; Lammers et al. 2001) might flow out from the Arctic Ocean without entering the deep basins. The remnant 2,350 km^3 $year^{-1}$ of runoff must enter the other basins. As 100 km^3 $year^{-1}$ of the net oceanic precipitation (2,000 km^3 $year^{-1}$) enters the Canada Basin then 1,900 km^3 $year^{-1}$ must enter the other basins. Waters exiting the Canada Basin are partitioned into ice (900 km^3 $year^{-1}$) and liquid water (2,300 km^3 $year^{-1}$) components, and the ratio of ice export to liquid water export is 0.4. Using the outflow boundary conditions of ice (2,460 km^3 $year^{-1}$) and liquid (5,600 km^3 $year^{-1}$) exiting the Arctic Ocean given by Serreze et al. (2006), the fluxes of waters exiting the other basins can thus be calculated according to their ice (1,550 km^3 $year^{-1}$) and liquid water (3,050 km^3 $year^{-1}$) components and the ratio of ice export to liquid water for the other basins is 0.5. This then allows closure of the budget (Fig. 14).

7.6 Summary

In this chapter we examined the large-scale distribution of freshwater in northern oceans (subarctic Pacific, Arctic and subarctic Atlantic) and found that the main storage reservoir for freshwater is the Beaufort Gyre of the Canada Basin, and therefore that small perturbations in export from this reservoir could well dominate interannual and decadal scale fluctuations downstream. We then focused on the Canada Basin, looking at gridded and observational data for variability in freshwater content and found that the dominant change since the 1990s was a southward shift in the location of the core of the Beaufort Gyre. However, the data available for this analysis are sparse. Only the repeat hydrography carried out in the southern Canada Basin since 2002 is of sufficient spatial resolution to make reliable comparisons. These 2002–2006 data show substantial interannual variability and it appears that the freshwater content has increased marginally during this time. We next used geochemical data to investigate freshwater components in the Canada Basin and found that meteoric water and the freshwater equivalent of Pacific water contribute almost equally to the total freshwater found in the upper 300 m, and that the net effect of sea-ice formation and melting removes ~30% of the annual supply. Finally we calculated volumes and residence times of the various source components that comprise the freshwater inventory of the Canada Basin, and then combined these findings with the overall freshwater budget of the Arctic Ocean compiled by Serreze et al. (2006) to arrive at a basin-wide description of source water fluxes. As storage within the basin is large and variable there is not

reason to suppose a priori that inflows and outflows must balance on annual to decadal time scales.

What are the existing knowledge gaps? Our estimates here are based on available data sets and it must be admitted that the uncertainty in many of these numbers is high and could be improved. For example, the historical context could be improved if the raw EWG data were made available, as this would allow direct comparisons between the past and present surveys and provide more insight about seasonal and interannual variability. Data from recent programs in the Canada Basin suggest circulation and storage within the Beaufort Gyre is highly variable and these findings demonstrate the value and importance of maintaining long-term observational programs. Ideally, the geographic reach of the observational program should be increased so that the entire Canadian Basin is surveyed and the northern reaches of the Beaufort Gyre determined. The basins immediately north of the Canadian Archipelago remain unexplored. Such extended surveys might also reveal if the shift in the Atlantic/Pacific water mass boundary away from the Lomonosov Ridge in the mid-1980s initiated a new permanent circulation mode or is only a transitory event on a yet-to-be determined time scale. As the majority of recent measurements have been collected during summer there is little known about the magnitude of seasonal variability, and moorings in the Canada Basin, both anchored and drifting, would provide such information. In terms of budgets, sea-ice estimates are rough calculations and require more detailed measurement and mapping to reflect recent and future changes. Data from a few moorings has shown that Bering Strait inflow has significant seasonal variability in all components (Woodgate et al. 2005) and therefore assigning a canonical transport value is a challenge. An array of moorings across Bering Strait would improve estimates of freshwater transport from the Pacific and include information about the Alaska Coastal and Anadyr currents.

The importance of identifying source components and how they are processed within the arctic basin becomes especially clear if one attempts to project what future freshwater exports would be under scenarios of global warming. The distinction is made all the more important by the fact that the ocean, with its longer residence times and recirculation rates, lags the atmosphere in response to climate forcing (cf. Peterson et al. 2006). How will climate change affect the processing and storage of freshwater components within the Arctic Basin, and thus quantitatively impact on export rates? Ice distillation (separation of ice and brines) accounts for ~30% of the freshwater export and therefore changes in the annual formation (thickness and extent) will impact the Arctic's freshwater budget. Changes in sea-ice cover may also trigger abrupt changes in air/ice/sea coupling (e.g. Carmack and Chapman 2003; Shimada et al. 2006). Changes in the supply of river water are also expected (Peterson et al. 2006; Déry and Wood 2005). Feedbacks among the interior Arctic and its marginal oceans will play a role (Dukhovskoy et al. 2004; Häkkinen and Proshutinsky 2004; Polyakov et al. 2007). Clearly, it is necessary to monitor not just the quantities of freshwater exiting the Arctic Ocean, but also their composition, their mode of formation and history, their mechanism of storage and release and the diverse physical constraints that limit their southward spreading as surface waters into

the North Atlantic. This last issue cannot be over emphasised because regional stratification within future subarctic seas will not increase (decrease) simply because river discharge increases (decreases) but instead is critically dependant upon the extent and dynamics of the reservoir to which it is confined.

Acknowledgements We are deeply indebted to the Captains and crews of the CCGS Louis S. St-Laurent for their undaunted efforts in completing our ambitious Canada Basin expeditions. We are also deeply indebted to Sarah Zimmerman and Bon van Hardenberg, who served as Chief Scientists, and the many dedicated technicians who carefully collected and analyzed samples.. Organisational support was provided by the National Centre for Arctic Aquatic Research Expertise, Fisheries & Oceans Canada. Partial funding for Eddy Carmack, Fiona McLaughlin and Michiyo Yamamoto-Kawai was provided by Fisheries and Oceans Canada, for Koji Shimada and Motoyo Itoh by the Japan Agency for Marine-Earth Science and Technology, and for Andrey Proshutinsky and Rick Krishfield by the National Science Foundation.

References

Aagaard K, Carmack EC (1989) The role of freshwater sea ice and other fresh waters in the Arctic circulation. Journal of Geophysical Research, 94, 14485–14498.

Aagaard K, Weingartner TJ, Danielson SL, Woodgate RA, Johnson GC, Whitledge TE (2006) Some controls on flow and salinity in Bering Strait. Geophysical Research Letters, submitted.

Anderson LG, Björk G, Holby O, Jones EP, Kattner G, Koltermann KP, Liljeblad B, Lindegren R, Rudels B, Swift J (1994) Water masses and circulation in the Eurasian Basin: Results frm the Oden-91 expedition. Journal of Geophysical Research, 99, 3273–3283.

Bacon S, Reverin G, Rigor IG, Snaith HM (2002) A freshwater jet on the east Greenland shelf, Journal of Geophysical Research, 107, doi: 10.1029/2001JC00935.

Bauch D, Schlosser P, Fairbanks R (1995) Freshwater balance and sources of deep and bottom water in the Arctic Ocean inferred from the distribution of $H_2{}^{18}O$, Progress in Oceanography, 35, 53–80.

Carmack EC (2000) The Arctic Ocean's freshwater budget: sources, storage and export. In: The Freshwater Budget of the Arctic Ocean. EL Lewis, EP Jones, P Lemke, TD Prowse and P Wadhams (eds.), Kluwer, Dordrecht, The Netherlands, pp. 91–126.

Carmack EC (2007) The alpha/beta ocean distinction: a perspective on freshwater fluxes, convection, nutrients and productivity in high-latitude seas, Deep-Sea Research II, 54, 2578–2598.

Carmack EC, Chapman DC (2003) Wind-driven shelf/Basin exchange on an Arctic Shelf: The joint roles of ice cover extent and shelf-break bathymetry. Geophysical Research Letters, 30, 1778, doi: 10 1029/2003GL017526.

Carmack EC,McLaughlin FA (2001) Arctic Ocean change and consequences to biodiversity: a perspective on linkage and scale, Memoirs of National Institute of Polar Research, Special Issue, 54, 365–375.

Carmack EC, Macdonald RW, Papadakis JE (1989) Water mass structure and boundaries in the Mackenzie Shelf Estuary, Journal of Geophysical Research, 94, 18043–18055.

Cenedese C, Linden PF (2002) Stability of a buoyancy driven coastal current at the shelf-break. Journal of Fluid Mechanics, 452, 97–121.

Chapman DC,Beardsley RC (1989) On the origin of shelf water in the Middle Atlantic Bight. Journal of Physical Oceanography, 18, 384–391.

Conkright ME, Antonov JI, Baranova O, Boyer TP, Garcia HE, Gelfeld R, Johnson D, Locarnini RA, Murphy PP, O'Brien TD, Smolyar I, Stephens C (2002) World Ocean Data Base 2001 vol.

1. In: Introduction. Sydney Levitus (ed.) NOAA Atlas NESDIS 42, US Government Printing Office, Washington, DC, 167 pp.
Dickson RR, Meincke J, Malmberg S-A,Lee AJ (1988) The "Great Salinity Anomaly" in the northern North Atlantic 1968–1982, Progress in Oceanography, 20, 103–151.
Dickson RR, Dye S, Karcher M, Meincke J, Rudels B, Yashayaev I (2007) Current Estimates of freshwater flux through Arctic and Subarctic seas. Progress in Oceanography, 73, 210–230, doi:10.1016/j.pocean.2006.12.003.
Dukhovskoy DS, Johnson MA, Proshutinsky A (2004) Arctic decadal variability: An auto-oscillatory system of heat and fresh water exchange. Geophysical Research Letters, 31, doi:10.1029/GL019023.
Déry SJ, Wood EF (2005) Decreasing river discharge in Northern Canada, Geophysical Research Letters, 32, doi:10.1029/GL022845.
Ekwurzel B, Schlosser P, Mortlock R, Fairbanks R, Swift J (2001) River runoff, sea-ice meltwater, and Pacific water distribution and mean residence times in the Arctic Ocean. Journal of Geophysical Research, 106, 9075–9092.
Environmental Working Group, Joint U.S.-Russian Atlas of the Arctic Ocean for the Winter Period [CD-ROM] (1998) National. Snow and Ice Data Center. Boulder, CO.
Falkner KK, O'Brien M, Carmack E, McLaughlin F, Melling H, Muenchow A, Jones EP (2006) Implications of nutrient variability in passages of the Canadian Archipelago and Baffin Bay for freshwater throughflow and local productivity. Journal of Geophysical Research, submitted.
Falck E, Kattner G, Budéus G (2005) Disappearance of Pacific Water in the northwestern Fram Strait. Geophysical Research Letters, 32, doi:10.1029/2005GL023400.
Griffiths RW (1986) Gravity currents in rotating systems. Annual Reviews in Fluid Mechanics 18, 59–89.
Guay CK, Falkner KK (1997) Barium as a tracer of Arctic halocline and river waters. Deep Sea Research, II, 44, 1543–1570.
Häkkinen S, Proshutinsky A (2004) Freshwater content variability in the Arctic Ocean. Journal of Geophysical Research, 109, doi:10.1029/2003JC001940.
Jones EP, Anderson LG, Swift JH (1998) Distribution of Atlantic and Pacific waters in the upper Arctic Ocean: implications for circulation. Geophysical Research Letters, 25, 765–768.
Jones EP, Swift JH, Anderson LG, Lipizer M, Civitarese G, Falkner KK, Kattner G, McLaughlin FA (2003) Tracing Pacific water in the North Atlantic, Journal of Geophysical Research, 108, doi:10.1029/2001JC001141.
Lagerloef G, Schmitt R (2006) Role of ocean salinity in climate and near-future satellite measurements, Eos 87.
Lammers RB, Shiklomanov AI, Vorosmarty CJ, Fekete BM, and Peterson BJ (2001) Assessment of contemporary Arctic river runoff based on observational discharge records, Journal of Geophysical Research, 106, 3321–3334.
Macdonald RW, Paton DW, Carmack EC, Omstedt A (1995) The freshwater budget and under-ice spreading of Mackenzie River water in the Canadian Beaufort Sea based on salinity and $^{18}O/^{16}O$ measurements in water and ice. Journal of Geophysical Research, 100, 895–919.
Macdonald RW, Mclaughlin FA, Carmack EC (2002) Freshwater and its sources during the SHEBA drift in the Canada Basin of the Arctic Ocean. Deep-Sea Research, II, 49, 1769–1785.
McLaughlin FA, Carmack EC, Macdonald RW, Bishop JKB (1996) Physical and geochemical properties across the Atlantic/Pacific front in the southern Canadian Basin. Journal of Geophysical Research, 101, 1183–1197.
McLaughlin FA, Carmack EC, Macdonald RW, Weaver AJ, Smith J (2002) The Canada Basin 1989–1995: Upstream events and far-field effects of the Barents Sea. Journal of Geophysical Research, 107, doi:10.1029/2001JC000904.
McLaughlin FA, Carmack EC, Macdonald RW, Melling H, Swift JH, Wheeler PA, Sherr BF, Sherr EB (2004) The joint roles of Pacific and Atlantic-origin waters in the Canada Basin, 1997–1998. Deep Sea Research, I, 51, 107–128.
McLaughlin FA, Carmack EC, Ingram RG, Williams WJ, Michel C (2006) Oceanography of the Northwest Passage, Chapter 31. In: The Sea Vol 14: The Global Coastal Ocean, Interdisciplinary

Regional Studies and Syntheses. AR Robinson, KH Brink (eds.), Harvard University Press, 1213–1244.
Melling H, Moore RM (1995) Modifications of halocline source waters during freezing on the Beaufort Sea shelf: evidence from oxygen isotopes and dissolved nutrients. Continental Shelf Research, 15, 89–113.
Östlund HG (1982) The residence time of the freshwater component in the Arctic Ocean. Journal of Geophysical Research, 89, 6373–6381.
Peterson BJ, McClelland J, Curry R, Holmes RN, Walsh JE, Aagaard K. (2006) Trajectory shifts in the Arctic and Subarctic freshwater cycle. Science, 313, 1061–1066.
Polyakov IV, Alexeev V, Belchansky GI, Dmitrenko IA, Ivanov V, Kirillov S, Korablev A, Steele M, Timokhov LA, Yashayaev I (2007) Arctic Ocean freshwater changes over the past 100 years and their causes. Journal of Climate, in press.
Proshutinsky A, Bourke RH, McLaughlin FA (2002) The role of the Beaufort Gyre in Arctic climate variability: Seasonal to decadal climate scales. Geophysical Research Letters, 29, 2100, doi:10.1029/2002gl015847.
Proshutinsky A, Yang J, Krishfield R, Gerdes R, Karcher M, Kauker F, Koeberle C, Hakkinen S, Hibler W, Holland D, Maqueda M, Holloway G, Hunke E, Maslowski W, Steele M, Zhang J (2005) Arctic Ocean Study: Synthesis of Model Results and Observations. Eos Transactions of the AGU, 86, 368, doi:10.1029/2005EO400003.
Richter-Menge J, Overland J, Proshutinsky A, Romanovsky V, Gascard JC, Karcher M, Maslanik J, Perovich D, Shiklomanov A, Walker D (2006) Arctic. In: State of the Climate in 2005. K.A. Shen (ed.), Special Supplement to the Bulletin of the American Meteorological Society, 87, S46–S52.
Rigor I, Wallace JM (2004) Variations in the age of Arctic sea-ice and summer sea-ice extent. Geophysical Research Letters, 31, doi:10.1029/2004GL019492.
Royer TC (1982) Coastal fresh water discharge in the Northeast Pacific. Journal of Geophysical Research, 87, 2017–2021.
Serreze MC, Barrett AP, Slater AG, Woodgate RA, Aagaard K, Lammers RB, Steele M, Moritz R, Meredith M, Lee C (2006) The large-scale freshwater cycle of the Arctic. Journal of Geophysical Research, 111(C11), doi:10.1029/2005JC003424.
Shimada K, McLaughlin FA, Carmack EC, Proshutinsky A, Nishino S, Itoh M (2004) Penetration of the 1990s warm temperature anomaly of Atlantic water in the Canada Basin. Geophysical Research Letters, 31, doi:10.1029/2004GL020860.
Shimada K, Kamoshida T, Nishino S, Itoh M, McLaughlin FA, Carmack EC, Zimmerman S, Proshutinsky A (2006) Pacific Ocean Inflow: influence on catastrophic reduction of sea ice cover in the Arctic Ocean. Geophysical Research Letters, 33, L08605, doi:10.1029/2005GL025624.
Smethie WM, Schlosser P, Bönisch G, Hopkins TS (2000) Renewal and circulation of intermediate water in the Canadian Basin observed on the SICEX 96 cruise. Journal of Geophysical Research, 105, 1105–1121.
Steele M, Ernold W (2007) Steric sea level change in the Northern Seas. Journal of Climate, 20, 403–417.
Steele M, Morison J, Ernold W, Rigor I, Ortmeyer M, Shimada K (2004) Circulation of summer Pacific halocline water in the Arctic Ocean. Journal of Geophysical Research, 109, doi:10.1029/JC002009.
Stigebrandt A (1984) The North Pacific: A global scale estuary. Journal of Physical Oceanography, 14, 464–470.
Swift JH, Aagaard K, Timokhov L, Nikiforov EG (2005) Long-term variability of Arctic Ocean waters: evidence from a reanalysis of the EWG data set. Journal of Geophysical Research, 110, doi:10.1029/2004JC002312.
Tully JP, Barber FG (1960) An estuarine analogy of the subarctic Pacific Ocean. Journal of the Fisheries Research Board of Canada 17, 91–112.
Walin G (1977) A theoretical framework for the description of estuaries. Tellus, 29, 128–136.
Weingartner TJ, Cavalieri DJ, Aagaard K, Sasaki Y (1998) Circulation, dense water formation and outflow on the northeast Chukchi shelf. Journal of Geophysical Research, 103, 7647–7661.

Wijffels SE, Schmitt RW, Bryden HL, Stigebrandt A (1992) Transport of freshwater by the oceans, Journal of Physical Oceanography, 22, 155–162.

Williams WJ, Weingartner TJ, Hermann AJ (2006) Idealized 3-dimensional modeling of seasonal variation in the Alaska Coastal Current. Journal of Geophysical Research, in revision.

Woodgate R, Aagaard K (2005) Revising the Bering Strait freshwater flux into the Arctic Ocean. Geophysical Research Letters, 32, doi:10.1029/2004GL021747.

Woodgate R, Aagaard K, Weingartner TJ (2005) Monthly temperature, salinity, and transport variability of the Bering Strait through flow. Geophysical Research Letters, 32, doi:10.1029/2004GL21880.

Yamamoto-Kawai M, Tanaka N, Pivovarov S (2005) Freshwater and brine behaviours in the Arctic Ocean deduced from historical data of $\delta^{18}O$ and alkalinity (1929–2002 A.D.). Journal of Geophysical Research, 100, doi:10.1029/2004JC002793.

Yamamoto-Kawai M, McLaughlin FA, Carmack EC, Nishino S, Shimada K (2008) Freshwater budget of the Canada Bain of the Arctic Ocean from geochemical tracer data. Journal of Geophysical Research, in press.

Zhang X, Zhang J (2001) Heat and freshwater budgets and pathways in the Arctic Mediterranean in a coupled ocean/ sea-ice model. Journal of Oceanography, 57, 207–234.